Structural Properties of Sodium Ion Implanted Poly(vinyl alcohol) Films

Narendra V. Bhat,[1] Mandar M. Nate,[1] Vaishali A. Bambole,[2] M. B. Kurup[3]

[1]*Bombay Textile Research Association, LBS Marg, Ghatkopar, Mumbai 400 086, India*
[2]*Physics Division, University Department of Chemical Technology, Matunga, Mumbai 400 019, India*
[3]*Tata Institute of Fundamental Research, Mumbai 400 005, India*

ABSTRACT: Poly(vinyl alcohol) (PVA) films were implanted with sodium ions at various energies and total doses. Modified films were characterized by Fourier transform IR (FTIR), UV–visible (UV–vis), X-ray diffraction (XRD), and scanning electron microscopy (SEM). From FTIR studies, it was evident that scission of the main chain occurred together with removal of hydrogen and hydroxyl groups. Sodium ions formed weak bonds with oxygen from the neighboring chains. UV–vis studies of implanted PVA showed increases in the absorbance values with the various energies and total doses. XRD studies revealed that, as the energy and total dose increased overall, the crystallinity decreased and new peaks at different 2θ values appeared. Changes in the crystallinity were also studied for thermally annealed PVA films in order to correlate and understand the phenomena of recrystallization due to ion implantation. The morphological features of the films were investigated by SEM. © 2005 Wiley Periodicals, Inc. J Appl Polym Sci 98: 276–283, 2005

Key words: poly(vinyl alcohol); ion implantation; Fourier transform IR; UV–visible; X-ray diffraction; scanning electron microscopy

INTRODUCTION

Most polymeric materials are normally dielectrics and many of them are good insulators. However, imparting electrical conduction to polymers is attractive because of several advantages and applications. Many electroactive polymers (polyacetylene, polypyrrole, polyaniline, etc.) have been reported recently.[1] These materials can be synthesized chemically or electrochemically and doped simultaneously. Many methods, such as chemical doping,[2] ion implantation,[3–5] and laser annealing,[6] have been tried to alter the polymer properties so that the material becomes conducting. A number of earlier studies[7,8] have established that ion implantation increases the conductivity of the polymers, but the specific changes in the polymer relating to the increase in conductivity and the mechanism of conduction are far from being well understood.

Ion implantation in polymers modifies the initial structure by crosslinking; scission; and formation of individual atoms, molecules, and molecule fragments.[9,10] This leads to changes in their properties like density, resistivity, optical absorption, molecular weight distribution, and solubility. The magnitude and nature of the changes depend on the composition of the polymer and the experimental parameters such as the ion energy, ion dose, and beam current. Ion implantation is used not only for doping but also for modifying their properties.[11,12] Changes in the chemical structure, conductivity, and electrochemical features of conducting polymers by ion implantation have been reported.[13–15]

For some applications, it becomes necessary to provide low electrical conductivity to polymeric materials. Electrostatic charges build up when polymeric films are used in carpets, packaging, belts, and so forth and can even cause severe shock in some cases. Thus, there is a great need for electrostatic dissipation of charges. The most important use is in packaging and processing of electronic circuit elements. Charge dissipation can occur by providing conducting paths. Therefore, it is essential to impart some electrical conductivity, which at present can be achieved by coating or blending with metallic powders. Conducting polymers (like polyaniline, polypyrrole, etc.) have been synthesized recently and several applications have been found. Mazurek et al. have reported that the conductivity of polyphenylele sulphide (PPS) can be enhanced by implantation of halogen, arsenic, and krypton ions.[16]

Poly(vinyl alcohol) (PVA) is an important polymer that is available in powder, film, and fiber forms. It is

TABLE I
Operating Conditions for Ion Implanter

Charge material: NaCl (Na$^+$)	Support gas: argon
Filament current: 25 A	Anode voltage: 200 V
Magnetic field: 50 G	Ambient pressure: 2.3×10^{-5} Torr
Arc current: 100–200 mA	Beam current: 2–3 μA
Vaccum of 2–3×10^{-5} Torr using two turbo molecular pumps	

used industrially for emulsification, sizing, and adhesives. Therefore, we thought it would be interesting to study the effect of ion implantation of PVA films. In the present investigation, PVA films were implanted with sodium ions at two different energies and different total doses. The implanted PVA films were characterized by Fourier transform IR (FTIR), UV–visible (UV–vis), X-ray diffraction (XRD), and scanning electron microscopy (SEM).

EXPERIMENTAL

PVA was obtained from S.D. Fine Chemicals (Boisar, Maharashtra, India). The PVA powder (2 g) was dissolved in 50 mL of deionized distilled water by heating at 80–90°C for 2 h. Films of PVA were obtained by pouring 4 wt % solution on a flat stainless steel plate. The thickness of the films was controlled by the volume of polymer solution. Each time 6–8 mL of polymer stock solution was poured on a stainless steel plate. Water was then evaporated by heating the plate in an oven at 70°C for 2 h. Films detached from the stainless steel plate were stored in a vacuum desiccator for further investigation. The thickness of the films was measured at five randomly selected places with a thickness gauge (accuracy = ±1 μm) and its mean value was found. The average thickness of the films was 45 μm.

For Na$^+$ ion implantation, the PVA films were cut into 2×2 cm^2 pieces and mounted on a circular metal disk with a 4-cm diameter. Samples were mounted in the chamber of a 400-kV ion-implanter machine at Tata Institute of Fundamental Research (Mumbai, India). This machine essentially consists of an ion source, ion extraction, beam injection to a mass analyzing magnet by an Einzel lens, high voltage for ion acceleration, focusing of an accelerated beam by an electrostatic quadrupole lens, and a beam deflector to switch the beam to different experimental beam lines. Typical operating data for sodium ion generation are given in Table I.

Sodium ions with varying energies are focused with the help of an electrostatic quadrupole lens to fall on 1 $\times$ 1 cm^2 of the PVA film. An energy of 100 keV was used to accumulate total doses of 2×10^{15} and 1×10^{16}

ions/cm^2 impinging on the PVA films. When an energy of 240 keV was used, a total dose of 2×10^{15} ions/cm^2 was allowed to fall on the film. Films were exposed for various durations, depending upon the energy, fluence rate, and total dose required. Implanted PVA film was brought to atmospheric pressure and carefully transferred to a vacuum desiccator for further characterization.
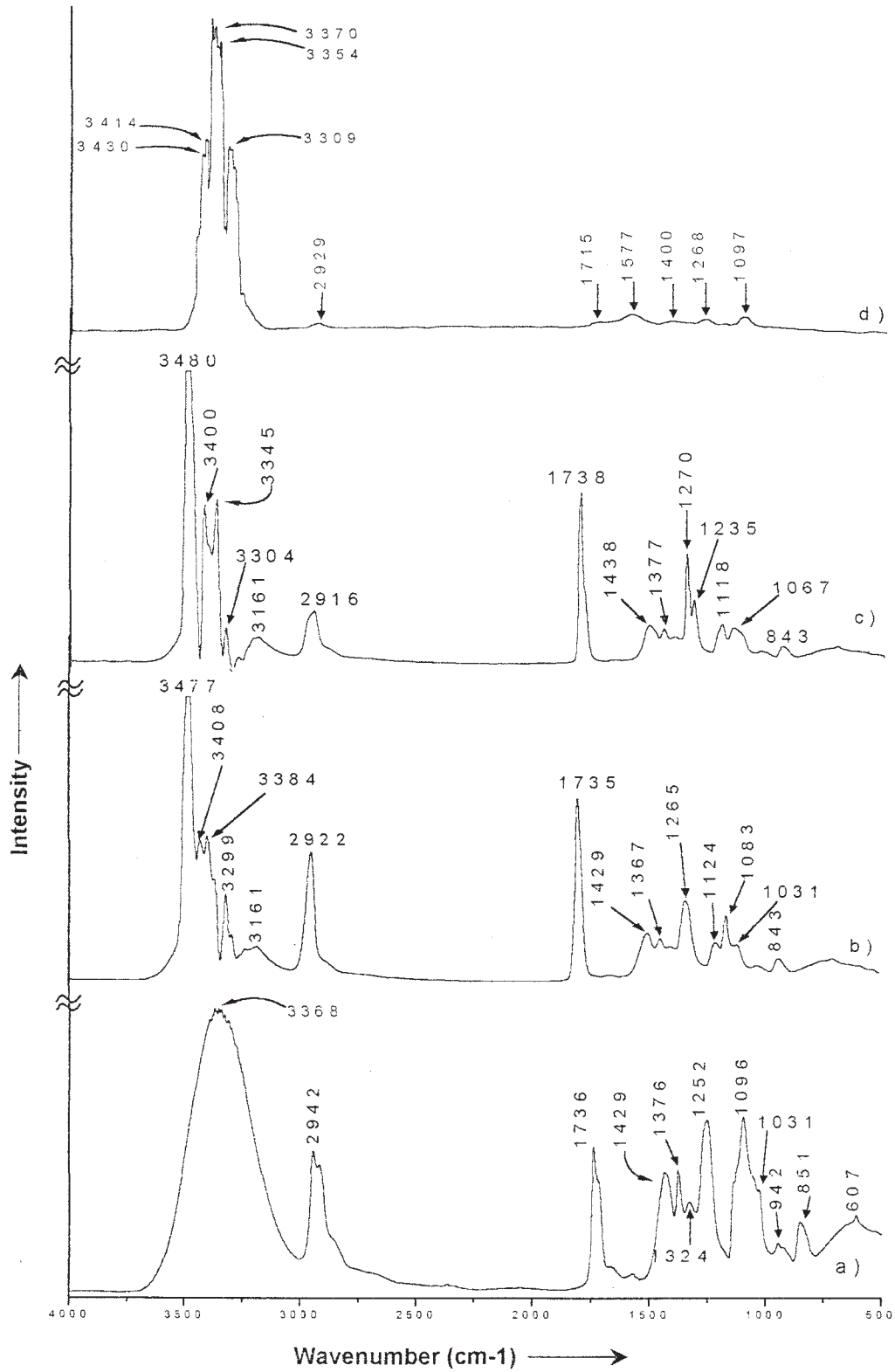
Sodium ion implanted PVA films were characterized by a Perkin–Elmer FTIR System 2000. Spectra were recorded from 4000 to 500 cm^{-1} with 25 scans and a resolution of 4 cm^{-1}. A UV–vis spectrum was obtained with a UV–vis 918 (GBC) spectrophotometer. X-ray studies were performed using an X-ray diffractometer (PW 1720, Philips) with 2θ varying from 10 to 40° with a step size of 0.01°.

The morphology of the PVA films was studied by SEM with a Jeol JSM-5400. The films were sputter coated with gold prior to examination. Micrographs were recorded at original magnifications of 100–5000. X-ray studies were performed on control and Na$^+$ ion implanted samples. In order to understand the nature of changes caused by ion implantation, the samples of control PVA were annealed at temperatures ranging from 50 to 150°C for 1–2 h.

RESULTS AND DISCUSSION

FTIR studies

Sodium ion implanted PVA films were studied by recording FTIR spectra. Figure 1 shows the FTIR spectra of control PVA and Na$^+$ ion implanted PVAs for two different energies and two different total doses. It can be seen that, in contrast to the control PVA film, ion implanted PVAs show significant changes in their respective vibration spectra (Table II). A broad band at 3368 cm^{-1} observed in control PVA films, which is due to O—H stretching vibration,[17,18] is affected considerably. This band in the spectra of implanted PVA samples, which were normalized and smoothened for intercomparison with the spectrum of control PVA, showed good resolution of bands. After ion implantation, significant splitting was observed in the O—H stretching vibration. In contrast to control PVA, where it was difficult to distinguish between H-bonded and non-H-bonded polymeric hydroxyl groups,[17] ion implanted samples show clear demarcations between the two types of hydroxyl groups. In the case of control PVA films, a broad band due to O—H stretching vibration, was centered at 3368 cm^{-1}. When the film was implanted with sodium ions with different total doses (same energy), significant changes in the O—H stretching vibrations were observed, as shown in Figure 2. A sharp absorption at 3480 cm^{-1}, which was due to single bridge intermolecular H bonding,[17] was observed. It is important to note that, in the case of

re 1 FTIR

Figure 1   FTIR spectra of control PVA and sodium ion implanted PVA films: control PVA (spectrum a), PVA film implanted at 100 keV with 2×10^{15} ions/cm^2 (spectrum b), PVA film implanted at 100 keV with 1×10^{16} ions/cm^2 (spectrum c), and PVA film implanted at 240 keV with 2×10^{15} ions/cm^2 (spectrum d).

TABLE II
FTIR Absorption Bands of Control and Na Ion Irradiated PVA Films

Wavenumber of control PVA film (cm^{-1})	Assignment	Wavenumbers for PVA films treated by Na ions (cm^{-1})		
		100 keV 2 × 10^{15} ions/cm^2	100 keV 1 × 10^{16} ions/cm^2	240 keV 2 × 10^{15} ions/cm^2
3368	OH stretching	3408	3400	3414
2942	CH$_2$ stretching	2922	2916	2929
1736	C=O stretching	1735	1738	1715
—	Conjugated C=C stretching	—	—	1577
1429	CH$_2$ bending	1429	1438	1400
1376	CH$_2$ wagging	1367	1377	—
1252	C—H wagging	1265	1270	1268
1143	C—C and C—O—C stretching	1124	1118	—
1096	C—O stretch and O—H bending	1083	1087	1097
1031	CO stretching	1031	1037	—
942	CH$_2$ rocking	—	—	—
851	C—C stretching	843	843	—

control PVA, this type of vibration did not seem to be present and, if at all present, it may have been very weak (Fig. 2). As the total dose was varied from 2
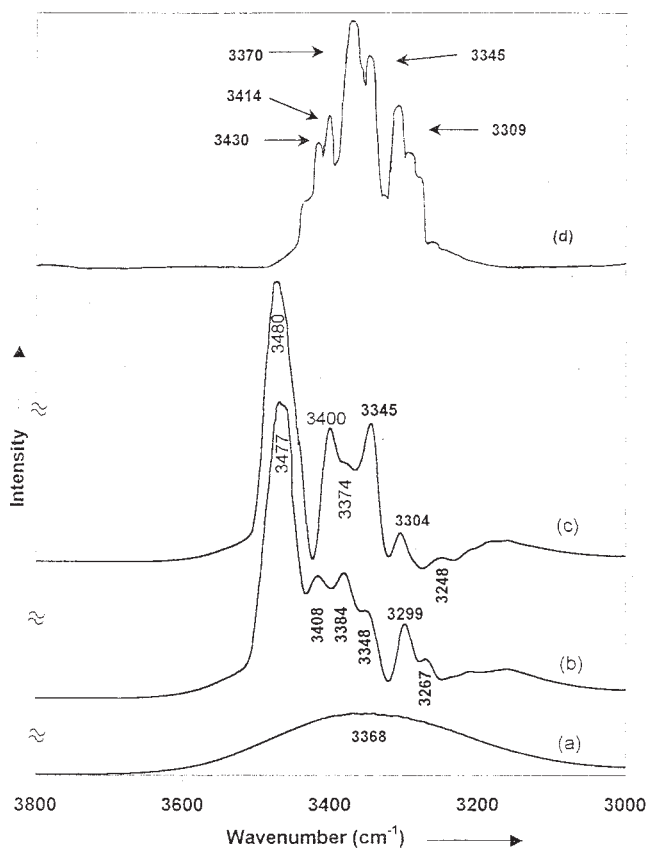

Figure 2 A comparison of the FTIR spectra of the O—H stretching vibration (3800–3000 cm^{-1}) of control PVA and sodium ion implanted PVA films: control PVA (spectrum a), PVA film implanted at 100 keV with 2 × 10^{15} ions/cm^2 (spectrum b), PVA film implanted at 100 keV with 1 × 10^{16} ions/cm^2 (spectrum c), and (d) PVA film implanted at 240 keV with 2 × 10^{15} ions/cm^2 (spectrum d).

× 10^{15} to 1 × 10^{16} ions/cm^2 and the energy was kept constant at 100 keV, significant changes were observed in the O—H stretching vibration. For the sample with a total dose of 2 × 10^{15} ions/cm^2, typical absorption peaks attributable to polymeric H bonds were observed at 3408, 3384, 3348, 3299, and 3267 cm^{-1}. However, when the total dose was increased to 1 × 10^{16} ions/cm^2, all these peaks were shifted to the lower wavenumber side (Fig. 2). Further, it can be seen from Figure 1 that, as the total dose was increased, the intensity of absorption in the 3480–3344 cm^{-1} region diminished considerably. In addition, the separation between 3399 and 3344 cm^{-1} decreased with an increase in the total dose from 64 to 55 cm^{-1}. A sharp peak centered at 3480 cm^{-1} was found to have decreased in its total area with the increase in the total dose. It is interesting to observe that, as the total dose was increased, the band at 3303 cm^{-1} became sharper. It is important to observe that the intensity of the —CH$_2$ stretching vibration at 2922 cm^{-1} of implanted PVA decreased with an increase in the total dose. In addition, we noted that the spectrum of Na$^+$ ion implanted films showed significant lowering in the intensity (including the crystalline peak) of the peak at 1096 cm^{-1}.

As the energy of the Na$^+$ ion increased to 240 keV, the FTIR spectra for films irradiated with a total dose of 2 × 10^{15} ions/cm^2 showed that the sharp peak previously centered at 3480 cm^{-1} completely disappeared and a set of new peaks were observed at 3430, 3414, 3370, 3345, and 3309 cm^{-1} (Fig. 2). It seems that bands due to polymeric H bonding in the 3400–3200 cm^{-1} range at lower energy become prominent at higher energy of implanted ions (240 keV) and the band due to single bridge intermolecular H bonding in the 3550–3450 cm^{-1} range disappeared at higher energy (Fig. 2).[17] These changes indicate that, at lower energies of implanted ions and lower total doses, the

| Wavenumber (cm^{-1})	Assignment	Wavenumbers for PVA films treated by Na ions (cm^{-1})		
		100 keV 2 × 10^{15} ions/cm^2	100 keV 1 × 10^{16} ions/cm^2	240 keV 2 × 10^{15} ions/cm^2
3480	Assigned to intermolecular H bond	3477	3480	—
3400	OH stretching (disrupted by Na)	3408	3400	3414
3374	Polymeric H bonding	3384	3374	3370
3345	Polymeric —OH bonding	3348	3345	3345

formation of single bridge intermolecular H bonding was observed and, as the energy is increased further, only polymeric H bonding was observed. It also shows the overall decrease in the intensity of the band attributable to —OH stretching, indicating removal of hydroxyl groups from the chain. The new peaks and their assignments are given in Table III. It is interesting to observe that the band near 2922 cm^{-1} is considerably diminished in intensity with the higher energy of 240 keV (Fig. 1). These changes indicate that the dehydrogenation of PVA film occurs after ion implantation at higher energy and fornation of a conjugated C≡C bond, which is evident from the new band at 1577 cm^{-1} (which is ascribed to a conjugated C≡C bond). The typical structural changes are indicated in the following structure:
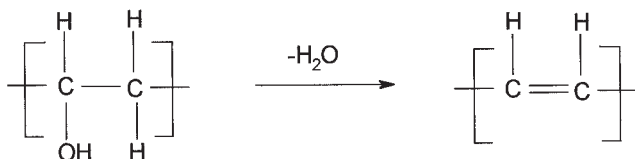
Thus, the PVA chains are broken and scission takes place. Similarly, hydrogen and the —OH functional group are separated from the PVA chains. Therefore, the degradation of PVA due to ion bombardment is evident.

The bombardment of PVA film with high energy Na$^+$ ions seems to bring about scission of the main chain, breaks the hydrogen and —OH bonds from the adjacent carbon atom, and leads to structural deformations. The XRD studies described in the next section revealed that the rupture of the polymeric chain is accompanied by heat generation. However, the question of how Na$^+$ ions become embedded in the structure remains partially unanswered. We therefore carried out studies on electrical conduction, and our preliminary study shows that there is an increase in the electrical conduction after the Na$^+$ ion implantation of PVA film. Further studies on solubility are in progress, but the preliminary results reveal that the irradiated films do not dissolve completely like the control film. Therefore, we propose structures that show Na$^+$ ions becoming involved in crosslinking the main chain.

The changes in the FTIR studies are striking in inferring the possible structural changes due to Na$^+$ ion implantation. In the case of PVA, it is well known that polymer chains are involved in intermolecular H bonding, as shown in structure (a). When the PVA film is implanted with high energy Na$^+$ ions, it is expected that it may rupture the polymeric chain and at the same time excess heat generated because of implantation may cause intermolecular H bonds to break and allow Na$^+$ ions to get involved in single bridge intermolecular H bonding, as shown in structure (b).

(a)   (b)
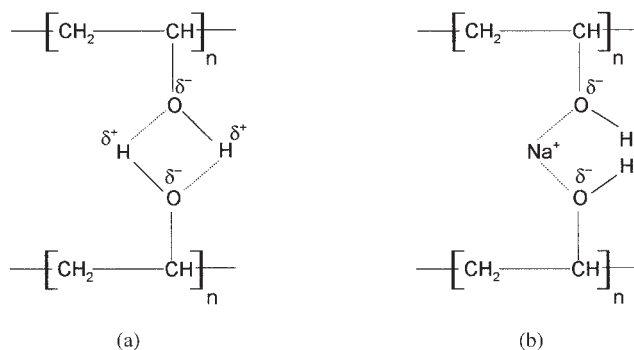
UV–vis studies

The PVA control film is colorless but becomes yellowish brown after irradiation when observed visually. Figure 3 shows UV–vis spectra of control and implanted PVA films. Note that control PVA is transparent in the 200–700 nm range. It is colorless and shows no absorption peaks in the visible region. In contrast, PVA films implanted with Na$^+$ ions showed significant absorption. The absorption intensity increases monotonically from 600 to 200 nm and is significant in the 400–200 nm region. It can be seen from Figure 3 that two broad absorption bands appear for irradiated samples: one at 350 nm and another sharp one at 250 nm.

The gradual increase in the absorption coefficients for the band at 350 nm is clear in the spectra (Fig. 3). This region is violet/blue in color, which is complimentary to yellow/orange. Therefore, the visual observation of a color change is supported by the spec-
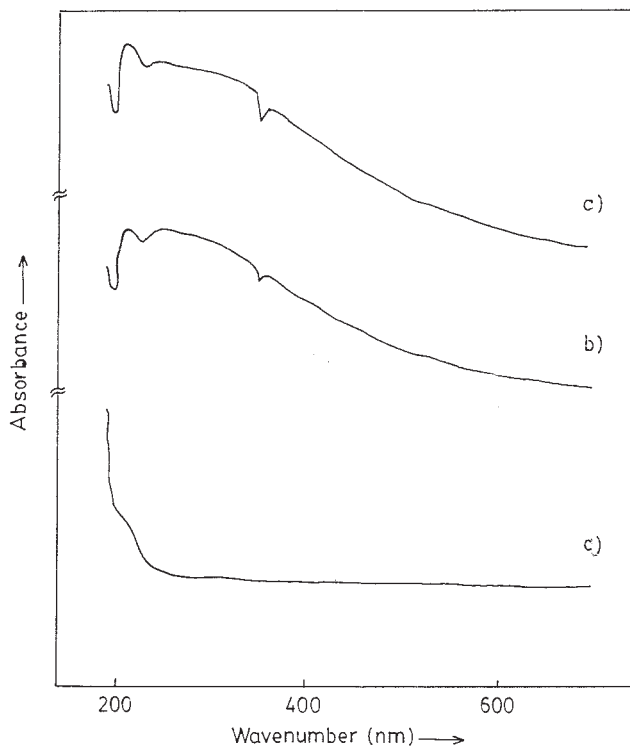
Figure 3 UV–vis spectra of control PVA and sodium ion implanted PVA films: control PVA (spectrum a), PVA film implanted at 100 keV with 2×10^{15} ions/cm^2 (spectrum b), and PVA film implanted at 100 keV with 1×10^{16} ions/cm^2 (spectrum c).

troscopic analysis and the observation of the absorption band at 350 nm. This coupled with the increase in the absorption at 250 nm (in the UV region) shows that some chromophores are formed. We observed that the absorbance was 2.1 for a total dose of 2×10^{15} ions/cm^2. When the dose was increased to 1×10^{16} ions/cm^2 (at 100 keV), the absorbance at 250 nm increased to 2.4. For the films irradiated with 240 keV ions with a total dose of 2×10^{15} ions/cm^2, the absorbance at 250 nm was 2.15.

Thus, as the total dose and energy was increased, the samples became nontransparent. In addition, a small peak appeared at 211 nm, which could possibly be due to conjugated double bonds.[19] It is thus inferred that the bombardment of high-energy ions causes scission of hydrogen and hydroxyl groups with subsequent formation of C=C. This conforms with the results of the FTIR spectra of implanted PVA.

XRD studies

The changes in the crystallinity due to ion implantation were investigated for PVA films by XRD studies. Figure 4 shows X-ray diffractograms of control and ion implanted PVAs at various total doses and energies. Control PVA exhibited a typical peak that ap-

peared at 2θ 18°. This peak was assigned to diffraction from a mixture of (101) and (10$\bar{1}$) planes.[20] The XRD patterns showed that the intensity for the peak at around 2θ 18° decreased gradually from control PVA to the PVA film implanted with Na$^+$ ions at an energy of 100 keV and a total dose of 2×10^{15} ions/cm^2, which further decreased for the PVA film implanted with Na$^+$ ions at a total dose of 1×10^{16} ions/cm^2. It was also noted that the position of the peak changed from 2θ 18° for control to 18.6° for the film with a dose of 2×10^{15} ions/cm^2 (100-keV energy). With an increase in the total dose to 1×10^{16} ions/cm^2, the peak still remained at 2θ 18.6°. However, for the total dose of 2×10^{15} ions/cm^2 but at an ion energy of 240 keV, the peak shifted to 2θ 19°. This indicates that the d value (interplanar spacing) for (101) planes decreases on irradiation. The PVA chains move closer together because of removal of the —OH in the process of irradiation and PVA gaining higher tacticity.

The percentage of crystallinity of control PVA film and PVA film implanted with Na$^+$ ions was calculated using the area under the curve method. The percentage of crystallinity of PVA decreased slightly from 56.29% for control PVA to 54.02% for the PVA implanted with Na$^+$ ions at a total dose of 2×10^{15} ions/cm^2 and 100-keV energy (Table IV). When the total dose was increased to 1×10^{16} ions/cm^2 (100-
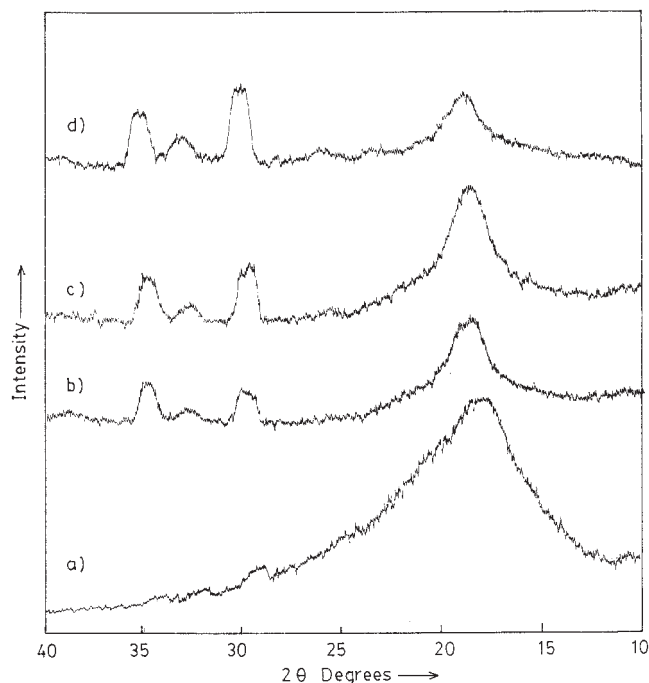
Figure 4 X-ray diffractograms of control PVA and sodium ion implanted PVA films: control PVA (spectrum a), PVA film implanted at 100 keV with 2×10^{15} ions/cm^2 (spectrum b), PVA film implanted at 100 keV with 1×10^{16} ions/cm^2 (spectrum c), and PVA film implanted at 240 keV with 2×10^{15} ions/cm^2 (spectrum d).

TABLE IV
Percentage Crystallinity of Control PVA Film and PVA Films Implanted with Sodium Ions at Different Energies and Total Doses

Sample	Crystallinity by intensity method (%)
Control PVA	89.91
Na$^+$ implanted PVA	
E = 100 keV, total dose = 2×10^{15} ions/cm^2	88.64
E = 100 keV, total dose = 1×10^{16} ions/cm^2	81.08
E = 240 keV, total dose = 2×10^{15} ions/cm^2	93.69

keV energy), then the percentage of crystallinity further decreased to 46.13%.

When the total dose of Na$^+$ ions was fixed at 2×10^{15} ions/cm^2 and the energy of the ions was increased from 100 to 240 keV, we observed that the percentage of crystallinity decreased from 56.02 to 36.96%. X-ray diffractograms of the PVA film implanted with Na$^+$ ions (100 keV, 2×10^{15} ions/cm^2) showed that three new peaks developed at 2θ 29.8°, 32.7°, and 34.8°. Such peaks were also present in the control PVA films, but the intensities were quite low. For control PVA films, peaks were observed at 29°, 32°, and 34° and their (*hkl*) indices were (201 + 20$\bar{1}$), (002), and (111), respectively.

The increase in the intensities of these peaks after irradiation is possibly attributable to growth of these planes that is caused by the rearrangement of molecules (due to scission of the main chain and removal of —H and —OH). This is accompanied by a decrease in the intensity of the main peak at 18°. Thus, the new structure grows because of disruption of the original lattice structure. This observation motivated us to calculate the percentage of crystallinity by a method based on the intensities of the diffraction peaks. These values are reported in Table IV, and they do not show much change after irradiation with Na ions. This is caused by the increase in the XRD peaks at higher angles, thereby giving higher resolution. Thus, even if the intensities of the peak at 18° decrease rapidly, the fall in the percentage of crystallinity is not substantial. However, if we use the single peak at 18° and the area under the curve method[21] for the calculations of percentage of crystallinity, rather than the formula based on the intensity,[22] then the decrease in the percent crystallinity is significant.

When the dose was raised to 1×10^{16} ions/cm^2 with 100-keV energy, these peaks shifted to 29.9°, 32.8°, and 34.9°, that is, at higher angles. Similarly, at a dose of 2×10^{15} ions/cm^2 at an energy of 240 keV, the peaks appeared at 30.2°, 33.1°, and 35.2°, that is, at higher angles. Thus, the *d* values decrease because the molecular chains become closer to each other. It is interesting to note that such peaks were also found in the

diffractograms of PVA films subjected to heat treatment for various temperatures (50–120°C). Thus, it appears that the energy of ions is partly dissipated as heat. The remaining part of the energy is used for removal of —OH groups and removal of the —H atom from the neighboring —CH$_2$ group, which leads to formation of H$_2$O and its subsequent removal. This also leads to crosslinking of PVA chains.

SEM studies

The morphology of control and irradiated films was studied by SEM, the features of which are depicted in Figure 5. Note that the morphology of the control PVA film is rather smooth with some particles. Such a structure is characteristic of the PVA surface and is agrees with earlier studies.[23] Figure 5(b) is a micrograph of PVA films irradiated with Na$^+$ ions at a dose of 2×10^{15} ions/cm^2. Some globular-like structures formed that are joined with deep grooved lines. The
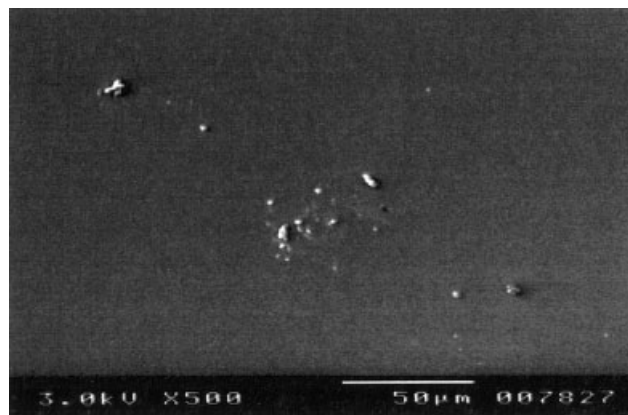
(a)
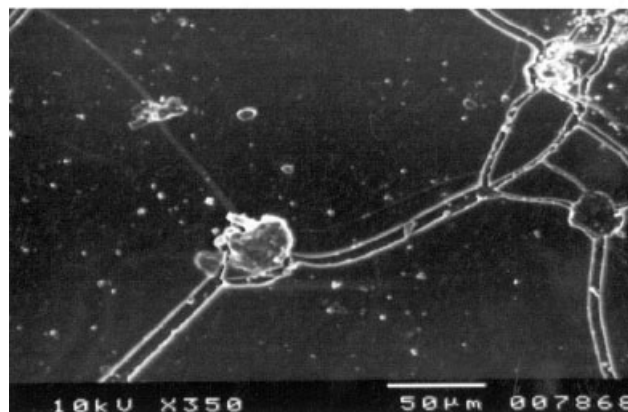
(b)

Figure 5 Electron micrographs of (a) control PVA and (b) PVA film implanted with sodium ions at 100 keV with a total dose of 2×10^{15} ions/cm^2.

average width of such lines is about 7 μm, whereas the length is more than 300 μm. It appears that such structures are because of some interaction of sodium ions with PVA and to defect formation.

CONCLUSIONS

PVA films implanted with sodium ions at 100- and 240-keV energies were significantly modified. Characterization using FTIR showed that scission of the main chain occurred together with removal of hydrogen and hydroxyl groups. Sodium ions formed weak bonds and some crosslinked product was formed. XRD studies revealed that the percentage of crystallinity decreased as the dose increased. The new diffraction peaks observed in the XRD led to the conclusion that part of the ion energy was released as thermal energy. The morphological studies using SEM conformed with other investigations. Thus, these studies revealed that the defect states were formed in molecular, macromolecular, and bulk structures when sodium ions were implanted.

References

1. Skotheim, T. A Handbook of Conducting Polymers; Marcel Dekker: New York, 1986; Vols. I, II.
2. Audenaert, M.; Gusman, G.; Deltour, R. Phys Rev B 1981, 24, 7380.
3. Kaplan, M. L.; Forrest, S. R.; Schmidt, P. H.; Venkatesan, T. J Appl Phys 1984, 55, 732.
4. Lee, E. H.; Rao, G. R.; Lewis, M. B.; Mansur, L. K. J Mater Res 1994, 9, 1043.
5. Balsubramanian, V.; Kelkar, D. S.; Kurup, M. B. Nucl Instrum Methods B 1996, 113, 257.
6. Schumann, M.; Sanerbrey, R. Appl Phys Lett 1991, 58, 428.
7. Bridwell, L. B.; Giedd, R. E.; Wang, Y. Q.; Mohite, S. S.; Jahnke, T.; Brown, I. M.; Bedell, C. J.; Sofield, C. J. Nucl Instrum Methods B 1991, 56/57, 656.
8. Zhu, J. L.; Lu, Z. M.; Yu, Z. W.; Guo, Y. P.; Ma, Z. T.; Beng, R. Z. Nucl Instrum Methods B 1994, 91, 469.
9. Muzzoldi, P.; Arnold, G. Ion Beam Modification of Insulators; Elsevier: Amsterdam, 1987.
10. Pignataro, S.; Marietta, G. In Metallized Plastics, 2nd ed.; Mittal, K. L., Ed.; Plenum: New York, 1991.
11. Moliton, A.; Duroux, J. L.; Froyer, G. Nucl Instrum Methods B 1998, 34, 450.
12. Kuczkowski, A.; Liwo, J. Synth Met 1987, 18, 575.
13. Koshida, N.; Hirayama, N. Nucl Instrum Methods B 1991, 59/60, 1292.
14. Schultze, J. W.; Jung, K. G.; Buchal, Ch. Nucl Instrum Methods B 1993, 80/81, 1076.
15. Lin, S.; Sheng, K.; Rong, T.; Bao, J.; Wang, W. M.; Zhou, Z. Y.; Zhu, X. F.; Yang, F. J. Nucl Instrum Methods B 1991, 59/60, 1257.
16. Mazurek, H.; Day, D. R.; Maby, E. W.; Abel, J. S.; Senturia, S. D.; Dresselhaus, M. S.; Dresselhaus, G. J Polym Sci Polym Phys 1983, 21, 537.
17. Bellamy, L. J. The lnfra-red Spectra of Complex Molecules; Chaucer Press Ltd.: Suffolk, UK, 1996.
18. Finch, C. A. Polyvinyl Alcohol Properties and Applications; Wiley: Bristol, UK, 1973.
19. Silverstein, R. M.; Bassler, G. C.; Morrill, T. C. Spectrometric Identification of Organic Compounds, 5th ed.; Wiley: Singapore, 1991.
20. Nishino, Y.; JohnManley, R. St. Macromolecules 1988, 21, 1270.
21. Alexander, L. E. X-Ray Diffraction Methods in Polymer Science; Wiley–Interscience: New York, 1969; Chapter 3.
22. Manjunath, B. R.; Venkataraman, A.; Stephen, T. J Appl Polym Sci 1973, 17, 1091.
23. Chen, S.-A.; Fang, W. G. Macromolecules 1991, 24, 1242.